

Variations in the 6.2 μm polycyclic aromatic hydrocarbon band in extragalactic sources

C. M. Canelo¹, D. A. Sales¹, & V. Avelaneda¹

¹ Instituto de Matemática, Estatística e Física, Universidade Federal do Rio Grande, Brazil e-mail: camcanelo@gmail.com

Abstract. The main reservoir of molecular organic material in space is in the form of polycyclic aromatic hydrocarbons (PAHs). They are of great astrochemical and astrobiological interest due to their potential to form prebiotic molecules. For instance, their simplest units with N atoms included in the aromatic rings, denominated Polycyclic Aromatic Nitrogen Heterocycles (PANHs), are involved in the production of Nucleobases. Normally present in Starburst (SB) galaxies, they have also been more frequently detected in active galaxy nuclei (AGNs), which suggest an inner dusty torus that can shield the radiation from the central black hole. In this work, we analyze the 6.2 μm PAH band of 175 SB-, AGN- and mixed-dominated galaxies, extracted from the IDEOS database. Our goal is to distribute the sources into the Peeters' A, B and C classes according to their profile peak positions. Variations in the profile can suggest some insight into the emitting PAH population or astrophysical conditions. Class A objects, for example, are predominant in 80% of the entire sample, which could indicate the presence of PAHs with nitrogen incorporation. Class B and C sources are more frequent in AGNs, which could be related to dusty material of the torus. The water ice feature at 6 μm and a second spectral feature between 6.4 and 6.7 μm are also present in 11 and 10 galaxies, respectively. Finally, the presence of PAHs in these sources strengthens the idea that organic (and prebiotic) molecules are ubiquitous throughout the Universe, even in distant galaxies. In this sense, the high-resolution observations of the James Webb Space Telescope (JWST) should improve our understanding on such subjects.

Resumo. O principal reservatório de material orgânico molecular no espaço está na forma de hidrocarbonetos policíclicos aromáticos (PAHs). Eles são de grande interesse astroquímico e astrobiológico devido ao seu potencial para formar moléculas pré-bióticas. Por exemplo, suas unidades mais simples com átomos de N incluídos nos anéis aromáticos, denominadas Heterociclos Policíclicos Aromáticos com Nitrogênio (PANHs), estão envolvidas na produção de Nucleobases. Normalmente presentes em galáxias Starburst (SB), eles também foram detectados com mais frequência em núcleos de galáxias ativas (AGNs), o que sugere um toro poeirento interno que pode blindar a radiação do buraco negro central. Neste trabalho, analisamos a banda PAH de 6.2 μm de 175 galáxias SB, AGN e misturadas, extraídas da base de dados CASSIS. Nosso objetivo é classificar as fontes nas classes A, B e C de Peeters de acordo com as posições dos picos de seus perfis. Variações no perfil podem fornecer informações sobre a população de PAHs emissores ou sobre as condições astrofísicas. Objetos da Classe A, por exemplo, são predominantes em 80% de toda a amostra, o que poderia indicar a presença de PAHs com incorporação de nitrogênio. Fontes das Classes B e C são mais frequentes em AGNs, o que poderia estar relacionado ao material poeirento do toro. A *feature* de gelo de água 6 μm e uma segunda *feature* espectral entre 6.4 e 6.7 μm também estão presentes em 11 e 10 galáxias, respectivamente. Finalmente, a presença de PAHs nessas fontes reforça a ideia de que moléculas orgânicas (e pré-bióticas) são onipresentes em todo o Universo, mesmo em galáxias distantes. Neste sentido, as observações de alta resolução do Telescópio Espacial James Webb (JWST) devem melhorar nossa compreensão sobre tais assuntos.

Keywords. galaxies: ISM – infrared: galaxies – ISM: molecules – astrochemistry – astrobiology

1. Introduction

Polycyclic aromatic hydrocarbons (PAHs) represent an effective arrangement for accumulating carbon in the Universe, being the dominant organic material in space (Ehrenfreund et al. 2006). Formed basically by carbon atoms distributed in various aromatic rings joined together, their robustness allows them to be among the most abundant molecular species that must have been transported almost intact to planets (Earth and Mars, for example), both by meteorite and comet falls and by interplanetary dust deposition (Ehrenfreund et al. 2002).

PAHs can constitute a stage in production channels of nitrogen-containing heterocyclic molecules (N-heterocycles), especially when their hydrogen or carbon atoms are replaced by nitrogen, giving rise to PANHs (polycyclic aromatic nitrogen heterocycles). In this sense, these molecules are of great astrochemical and astrobiological interest because they may have played a prebiotic role in the origins of life at stages preceding the RNA/DNA world (Ehrenfreund et al. 2006), both on Earth and in other astrophysical environments.

About 15% of the carbon in the interstellar medium (ISM) is found in the form of PAHs, and the emission in mid-infrared (MIR) bands is dominated by the bands of this class of molecules

(Joblin et al. 2002), known as AIBs (Aromatic Infrared Bands). Moreover, PAHs can be responsible for up to 50% of the luminosity in the MIR, with the most intense emission bands at 3.3, 6.2, 7.7, 8.6, 11.2, and 12.7 μm (Li 2004). This high luminosity also allows PAHs to be observed in high redshift objects, in which they can dominate the emission in the infrared spectrum (Papovich et al. 2006; Teplitz et al. 2007). To date, the highest redshift at which PAH emission has been detected is $z = 4.055$ in the submillimeter galaxy GN20 (Riechers et al. 2014).

Variations in the profiles of PAH bands are present in various astrophysical sources, both galactic and extragalactic. Such variations were first studied by Peeters et al. (2002), who divided the spectral region in the MIR from 6 to 9 μm into three classes – A, B and C – according to the central peak position of the bands. Later, Van Dierendonck et al. (2004) expanded the classification to the 3.3 and 11.2 μm bands and revealed a correlation between the classes and their respective profiles. The differences between profiles may arise from various factors that include local physical conditions, the cumulative effect of processing in the regions where the emission originated and/or characteristics of the PAH population, such as family composition, molecular size, charge, geometry and heterogeneity (Sales et al. 2010, 2013; Ruschel-

Dutra et al. 2014; Canelo et al. 2018). In this way, the study of variations and classes of PAHs can help better understand the physical and chemical conditions of various astrophysical environments.

Shannon & Boersma (2019), for example, suggested a possible evolutionary cycle of PAHs based on the stellar life cycle, in which each evolutionary stage of the star is related to distinct PAH populations. It is possible that this evolutionary cycle can also be extrapolated to an extragalactic view. Canelo et al. (2018) studied the 6.2 μm of 155 galaxies with starburst-dominated emission, that is, galaxies with intense star formation where strong PAH emission is expected. The already-reduced spectra of these galaxies were extracted from the Spitzer/IRS ATLAS project (Hernández-Caballero & Hatziminaoglou 2011). With redshifts up to 2.5, the galaxies had this band distributed among Peeters' classes and showed a predominance of Class A objects that decreases with increasing redshift. Similar trends were also found for the other 7.7 and 8.6 μm bands for the same sample (Canelo et al. 2021) and suggest a possible temporal evolution of PAHs.

This is the first time that a study of PAHs (together with Peeters' classes) is conducted with robust statistics for a large number of extragalactic sources with a wide variety of redshifts. Therefore, expanding this study to other PAH bands and, especially, to other types of objects such as AGNs (Active Galactic Nuclei) can reveal new information about PAH populations and their relationship with different astrophysical objects, and may even contribute to increasing our understanding of galaxy evolution in the cosmological context.

2. Data Selection

In order to expand our previous analysis (e.g. Canelo et al. 2018, 2021), we selected the 155 spectra from Infrared Database of Extragalactic Observables from Spitzer¹ (IDEOS, Spoon et al. 2022). The IDEOS database provides mid-infrared diagnostics and spectra for more than 3,330 galaxies/galactic nuclei from spectroscopic measurements obtained by the Infrared Spectrograph (IRS) on Spitzer. The classification of the sources into AGN- and SB-dominated galaxies was based on a diagnostic diagram that combined the ice-corrected equivalent width of the 6.2 μm PAH feature with the silicate strength into a grid of 3×3 mid-IR classes, from 1A to 3C. (see Spoon et al. 2022, for more details). We then divide our sample in three types: SB, corresponding to class 1C PAH-dominated spectra typical for starburst galaxies; AGN 1, corresponding to class 1A objects with a hot-dust-dominated spectrum typical for AGNs; and the mixed-dominated objects are the galaxies in between these classes.

3. Data analysis and results

Before fitting the profile of the PAH band, it is necessary to subtract the spectral contributions of the continuum from the original spectra. The continuum of the galaxies can be fitted through decomposition by splines with anchor points around 5.0, 5.4, 5.5, 5.8, 6.6, 7.0, 8.2, 9.0, 9.3, 9.9, 10.2, 10.5, 10.7, 11.7, 12.1, 13.1, 13.9, 14.7 and 15.0 μm depending on the spectral coverage of each object (for example, Peeters et al. 2017).

The anchor point at 8.2 μm has been widely discussed. Around that wavelength, there is a broad emission profile, a sort of bump. It can be caused by dust grains and be extracted from the spectrum, which facilitates the analysis of the 7.7 and

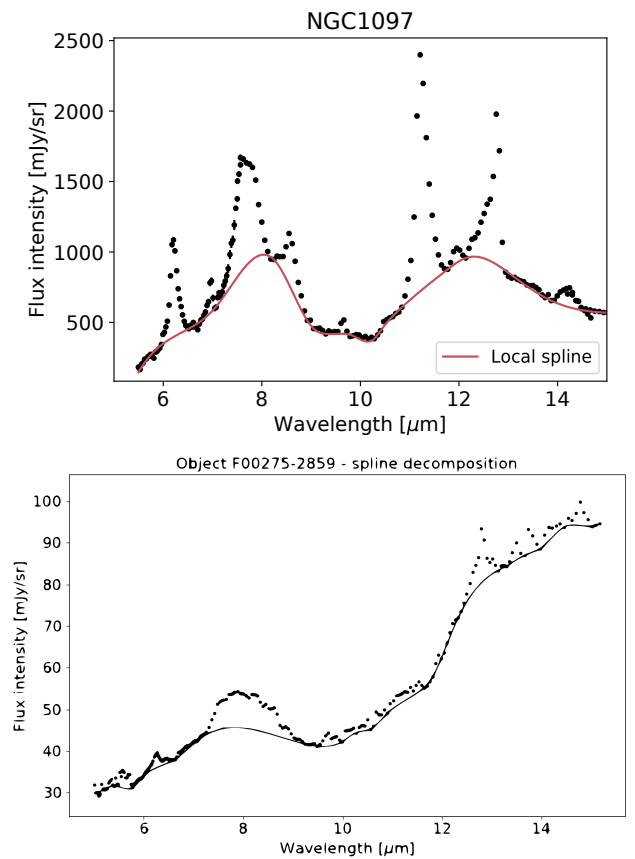


FIGURE 1. Decomposition by spline of the continuum emission represented by the red and/or continuous line. The data are represented by the points with vertical error bars as uncertainties. The two situations with or without the inclusion of the anchor point at 8.2 μm are shown.

8.6 μm PAH bands (for example, Brandl et al. 2006). On the other hand, it can be considered PAH emission that, therefore, could not be considered as part of the continuum emission (for example, Peeters et al. 2017). These two approaches are shown in Fig. 1. The first galaxy is dominated by *starbursts* and had the bump included in the continuum subtraction (Canelo et al. 2021). In the case of the second galaxy, dominated by AGN, it is easy to notice the difference between the spectra and how the bump should be considered separately.

After the continuum subtraction, the PAH band can be fitted with Gaussian through the PYTHON algorithm developed by Canelo et al. (2018), which propagates the uncertainties and accommodates constraints on the parameters in its new version. An example of this procedure can be seen in Fig. 2. Some sources can present a water-ice absorption at 6.0 μm . In our sample, eleven galaxies shown such feature but the PAH band fit has not suffered any interference. This PAH band can also present a profile with a tail at redder wavelengths, mainly in Class A objects. This feature can be either an effect of the peak asymmetry as well as weaker emission from other molecules such as C_{60}^+ or PAHs with aliphatic structures (Canelo et al. 2018, and references therein).

With the fitted profiles, it is possible to classify the bands into Peeters' classes and verify their distribution along the redshifts of the galaxies. The preliminary results indicate a predominance of Class A sources, corroborating our previous work. In fact, 80% of the entire sample, especially SB- and mixed-dominated objects, received the A classification. This could indicate the presence

¹ <http://ideos.astro.cornell.edu/>

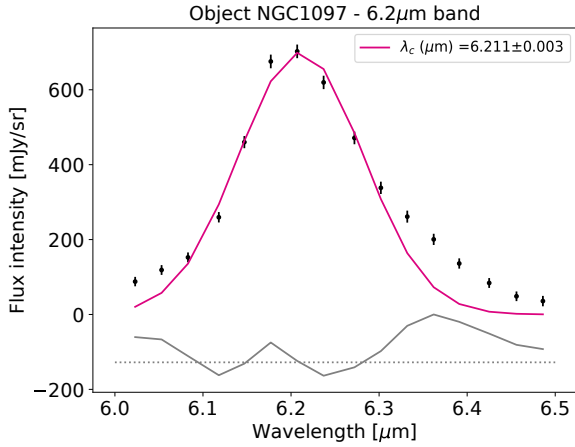


FIGURE 2. Example of a 6.2 μm fit result for object NGC 1097. The solid gray lines represent the fit residuals shifted for better visualization. (Canelo et al. 2018, 2021).

of PANH molecules in harsh environments together with AGNs. We are still selecting additional galaxies to improve the diversity of galaxy types, focusing on AGN objects. These are expected to show more examples of Class C objects, which could be related to the dusty material of those galaxies.

4. Conclusion

In this work, we analyzed 175 galaxies from the IDEOS database, divided on SB, AGN 1 and mixed-dominated objects. After continuum subtraction, their 6.2 μm bands were fitted and distributed into the Peeters' classes. As expected, the preliminary results show that Class A objects dominate the sample and Class C appears more frequently in the AGN 1 objects. Although further research is need, this work can be used as a guide to new observations and analysis with the James Webb Space Telescope².

Acknowledgements. CMC acknowledges the support of Coordenação de Aperfeiçoamento de Pessoal de Nível Superior - Brasil (CAPES) - Finance Code 001 - Brazil, process number 88887.967338/2024-00.

References

- Brandl, B. J. et al. 2006, *ApJ*, 653, 1129
 Canelo, C., Friaça, A., Sales, D., Pastoriza, M. & Ruschel-Dutra, D. 2018, *MNRAS*, 475, 3746
 Canelo, C., Sales, D., Friaça, A., Pastoriza, M. & Menéndez-Delmestre, K. 2021, *MNRAS*, 507, 6177
 Ehrenfreund, P., Irvine, W., Becker, L. et al. 2002, *Rep. Prog. Phys.*, 65, 1427
 Ehrenfreund, P., Rasmussen, S., Cleaves, J. & Chen, L. 2006, *Astrobiology*, 6, 490
 Hernán-Caballero, A. & Hatziminaoglou, E. 2011, *MNRAS*, 414, 500
 Joblin, C., Léger, A. & Martin, P. 2002, *ApJ*, 393, L79
 Li, A. 2004, *ASP Conf. Ser.*, 309, 417
 Papovich, C. et al. 2006, *ApJ*, 640, 92
 Peeters, E., Hony, S., Van Kerckhoven, C. et al. 2002, *A&A*, 390, 1089
 Peeters, E., Bauschlicher, C., Allamandola, L. et al. 2017, *ApJ*, 836, 198
 Riechers, D. et al. 2014, *ApJ*, 786, 31
 Ruschel-Dutra, D., Pastoriza, M., Riffel, R., Sales, D. & Winge, C. 2014, *MNRAS*, 438, 3434
 Sales, D., Pastoriza, M. & Riffel, R. 2010, *ApJ*, 725, 605
 Sales, D., Pastoriza, M., Riffel, R. & Winge, C. 2013, *MNRAS*, 42, 2634
 Shannon, M. & Boersma, C. 2019, *ApJ*, 871, 124
 Spoon, H. et al. 2022, *ApJS*, 259, 37
 Teplitz, H. et al. 2007, *ApJ*, 659, 941
 Van Dienenhoven, B. et al. 2004, *ApJ*, 611, 928

² <https://webb.nasa.gov/>